Physiological and transcriptional profiling of surfactin exerted antifungal effect against *Candida albicans*

Running headline: Effects of surfactin against *C. albicans*

Ágnes Jakab[1,2], Fruzsina Kovács[2,3], Noémi Balla[2,3], Zoltán Tóth[2,3], Ágota Ragyák[1,4], Zsófi Sajtos[4], Kinga Csillag[1], Csaba Nagy-Köteles[1], Dániel Nemes[5], István Pócsi[1], László Majoros[2], Ákos T. Kovács[6], Renátó Kovács[2,7*]

[1]Department of Molecular Biotechnology and Microbiology, Institute of Biotechnology, Faculty of Science and Technology, University of Debrecen, Debrecen, Hungary

[2]Department of Medical Microbiology, Faculty of Medicine, University of Debrecen, Debrecen, Hungary

[3]Doctoral School of Pharmaceutical Sciences, University of Debrecen, Debrecen, Hungary

[4]Department of Inorganic and Analytical Chemistry, Agilent Atomic Spectroscopy Partner Laboratory, University of Debrecen, Debrecen, Hungary

[5]Department of Pharmaceutical Technology, Faculty of Pharmacy, University of Debrecen, Debrecen, Hungary.

[6]Bacterial Interactions and Evolution Group, DTU Bioengineering, Technical University of Denmark, Kongens Lyngby, Denmark.

[7]Faculty of Pharmacy, University of Debrecen, Debrecen, Hungary

*Corresponding author: Renátó Kovács; Department of Medical Microbiology, Faculty of Medicine, University of Debrecen, 4032 Debrecen, Nagyerdei krt. 98., Hungary, Phone: 00-36-52-255-425; e-mail: kovacs.renato@med.unideb.hu

Abstract

Given the risk of *Candida albicans* overgrowth in the gut, novel complementary therapies should be developed to reduce fungal dominancy. This study highlights the antifungal characteristics of a *Bacillus subtilis*-derived secondary metabolite, surfactin with high potential against *C. albicans*. Surfactin inhibited the growth of *C. albicans* following a 1-hour exposure, in addition to reduced adhesion and morphogenesis. Specifically, surfactin did not affect the level of reactive oxygen species but increased the level of reduced glutathione. Surprisingly, ethanol production enhanced following 2 hours of surfactin exposure. Surfactin treatment caused a significant reduction in intracellular iron, manganese and zinc content compared to control cells, whereas the level of copper was not affected. Alongside these physiological properties, surfactin also enhanced fluconazole efficacy. To gain detailed insights into the surfactin-related effects on *C. albicans*, genome-wide gene transcription analysis was performed. Surfactin treatment resulted in 1390 differentially expressed genes according to total transcriptome sequencing (RNA-Seq). Of these, 773 and 617 genes with at least a 1.5-fold increase or decrease in transcription, respectively, were selected for detailed investigation. Several genes involved in morphogenesis or related to metabolism (e.g., glycolysis, fermentation, fatty acid biosynthesis) were down-regulated. Moreover, surfactin decreased the expression of *ERG1*, *ERG3*, *ERG9*, *ERG10* and *ERG11* involved in ergosterol synthesis, whereas genes associated with ribosome biogenesis and iron metabolism and drug transport-related genes were up-regulated. Our data demonstrate that surfactin significantly influences the physiology and gene transcription of *C. albicans*, and could contribute to the development of a novel innovative complementary therapy.

Importance

Although gut colonization by *Candida albicans* can be considered normal, it may be associated with intestinal diseases. Furthermore, *Candida* dominance in the gut may pose a potent risk for systemic candidiasis, especially for immunocompromised individuals. In recent years, interest has been growing for the use of *Bacillus subtilis* as a safe and effective probiotic for human healthcare. Surfactin is a *B. subtilis*-derived lipopeptide with potential antifungal activity; however, the mechanism underlying this remains unknown. In this study, surfactin negatively affected the adherence, morphogenesis and metabolism of *C. albicans* and increased ethanol production. These were associated with a reduction in intracellular iron, manganese and zinc while the copper content was not affected. Alongside these physiological modulations, surfactin also had a potent synergistic effect on fluconazole. Our results provide a definitive explanation for the surfactin-related antifungal effect of *B. subtilis*; furthermore, these data provide a good basis for future probiotic development.

Keywords: *Candida albicans*, surfactin, probiotic, transcriptomics, metal, *Bacillus subtilis*

Introduction

Molecular typing of *Candida albicans* isolates showed high similarity between those isolated from blood and isolates colonizing the gastrointestinal tract proving that gut might be one of the most important sources of invasive candidiasis (1-2). Microbial dysbiosis and *Candida* dominance in the gut can be considered as a potent risk for systemic candidiasis, especially in patients treated with cytotoxic agents that disrupt the intestinal mucosa (3). Thus, it is important to develop and introduce new supportive and complementary therapeutic strategies in order to reduce the overgrowth of *Candida* cells in the gut. The administration of various probiotics may be a useful approach in this context (4-6). Different species from the *Lactobacillus* and *Bifidobacterium* genera are the most frequently used probiotics. Nevertheless, other potential probiotic species have also been shown to be effective for the treatment of gastrointestinal candidiasis (7).

In the last decade, there has been increasing interest in the use of *Bacillus subtilis* strains as safe and effective probiotics for human healthcare (7). On the one hand, *B. subtilis* spores modulate the immune response of the host; on the other hand, the vegetative form can release enzymes, antioxidants and vitamins to support digestion. It is important to emphasize that *B. subtilis*-derived exopolysaccharides have relevant immunomodulatory effect, which may prevent inflammatory disease induced by enteric pathogens (8-9). Moreover, several strains of *B. subtilis* can secrete antimicrobial compounds, promoting the optimal microbial balance (10-12). Generally, members of the *B. subtilis*-species complex are potent source for natural products with anti-fungal compounds, including anti-*Candida* activity (13). Among these natural products, surfactin is a *B. subtilis*-derived cyclic lipopeptide that shows activity against gram-positive bacteria and has a wide range of targets, so it is difficult for microorganisms to develop drug resistance against it (10-12). Previous studies showed that its

93 oral half-lethal dose in mice exceeded 5000 mg/kg, and that acute toxicity was low or lacking
94 (14).
95 Recent studies revealed that surfactin has an effect on yeasts; furthermore, it effectively
96 decreases the adhesion of *C. albicans* and its hydrophobicity (15-18). Nevertheless, the effect
97 of surfactin on *C. albicans* has not been sufficiently investigated and the underlying
98 mechanisms of surfactin-induced effects remain unknown. Understanding how surfactin can
99 influence the physiological and genetic properties of *C. albicans* would be pivotal in further
100 probiotic development. To gain further insights into its previously observed inhibitory
101 potential, we report the effect of surfactin on cell growth, adhesion, virulence, metabolism,
102 and intracellular metal content, in addition to the genome-wide gene expression changes
103 caused by surfactin exposure as determined using total transcriptome sequencing (RNA-Seq).
104

Materials and methods

Fungal strain, culture media and epithelial cell line

The SC5314 *C. albicans* wild-type reference strain was maintained and cultured on yeast extract-peptone-dextrose (YPD) (VWR, 2% glucose, 2% peptone, 1% yeast extract with or without 2% agar) as described previously (19). Susceptibility experiments to fluconazole (Merck, Budapest, Hungary) and surfactin was determined in RPMI-1640 (with L-glutamine and without bicarbonate, pH 7.0 with MOPS; Merck, Budapest, Hungary). For toxicity and adhesion experiments, the Caco-2 epithelial cell line was obtained from the European Collection of Cell Cultures (ECACC) (Salisbury, United Kingdom) and cultured as described previously by Nemes et al. (20). Briefly, cells were grown in plastic cell culture flasks in Dulbecco's modified Eagle's medium (DMEM) supplemented with 3.7 g/l $NaHCO_3$, 10% (vol/vol) heat-inactivated fetal bovine serum, a 1% (vol/vol) non-essential amino acid solution, 0.584 g/l L-glutamine, 4.5 g/l D-glucose, 100 IU/ml penicillin, and 100 mg/l streptomycin at 37°C in the presence of 5% CO_2. The cells were maintained by regular passaging, and glutamine was supplemented with GlutaMAX. Cells between passages 20 and 40 were used for adhesion and toxicity experiments (20).

Toxicity experiments

Concentrations of 16 mg/l, 32 mg/l, 64 mg/l, 128 mg/l and 256 mg/l surfactin were evaluated regarding toxicity to Caco-2 cell line using a 3-(4,5-dimethyl-2-thiazolyl)-2,5-diphenyl- 2H-tetrazolium bromide (MTT) assay (Merck, Budapest, Hungary) and xCELLigence real-time cell analysis (ACEA Biosciences, Inc., San Diego, CA, USA), where none of them caused relevant toxicity (19–20). A final concentration of 128 mg/l surfactin (Merck, Budapest, Hungary) was used in our experiments, corresponding to the average surfactin production of various *B. subtilis* strains (21).

130

131 **Growth assay**

132 *C. albicans* pre-cultures were grown in 5 ml YPD medium at 37ºC for 18 hours, diluted to an
133 optical density of 0.1 (OD_{640}) with YPD then grown further at 37ºC and at 2.3 Hz shaking
134 frequency. Following a 4-hour incubation period, some cultures were supplemented with 128
135 mg/l surfactin, and microbial growth was followed by measuring changes in optical density at
136 640 nm and dry cell mass (DCM) (19,22). Samples were taken at 1 hour for RNA isolation
137 and for measurement of redox changes, phospholipase, lipase and extracellular protease
138 activity. Two- and 4-hour surfactin exposures were used to determine glucose consumption
139 and ethanol production. The glutathione and intracellular metal contents were determined
140 following 4 hours of surfactin treatment.
141 Morphological changes exerted by surfactin were examined after 4, 5, 6 and 8 hours of
142 incubation at 37 °C using a Zeiss Axioskop 2 mot microscope coupled with a Zeiss Axiocam
143 HRc camera using the phase-contrast technique (23).
144 For all experiments, statistical analyses were performed between control and surfactin-treated
145 cultures using the paired Student's *t* test. Significance was defined as a p value of < 0.05.

146

147 **Phospholipase, esterase and extracellular protease activity**

148 Extracellular phospholipase production by surfactin-treated (128 mg/l) and untreated *C.*
149 *albicans* cells was investigated on egg yolk medium [4% glucose, 1% peptone, 5.85% NaCl,
150 0.05% $CaCl_2$, and 10% (vol/vol) sterile egg yolk emulsion, 1.5% agar]. Esterase activity was
151 determined on Tween-20 medium [1% peptone, 0.5% NaCl, 0.01% $CaCl_2 \times 2H_2O$, 1%
152 (vol/vol) Tween-20 (Merck, Budapest, Hungary), 2% agar]. Aspartic proteinase secretion was
153 evaluated on solid bovine serum albumin medium [0.02% $MgSO_4 \times 7H_2O$, 0.25% K_2HPO_4,

0.5% NaCl, 0.1% yeast extract, 2% glucose and 0.25% bovine serum albumin (Merck, Budapest, Hungary), 2% agar].

To assess the production of virulence-related enzymes, 5-µl suspensions of *Candida* cells (1×10^7 CFU/ml) were inoculated onto agar plates as described previously (24). Colony diameter and precipitation zones on egg yolk and Tween-20 plates and clear areas on bovine serum albumin media (Pz) were measured after 7 days of incubation at 37°C (22). Enzyme activities were measured in three independent experiments and are presented as means with standard deviations.

Determination of glucose consumption and ethanol production

Aliquots of *C. albicans* culture media were collected by centrifugation (5 min, 4000×g, 4°C) following 2 and 4 hours of surfactin exposure. Changes in the glucose contents of the *C. albicans* supernatants were determined using the glucose oxidase assay described by Jakab et al. (25).

The concentration of ethanol in culture media was determined by headspace gas chromatography (HS-GC-FID system, PerkinElmer GC, Clarus 680 with PerkinElmer TurboMatrix 40 Trap Headspace Sampler, FID with helium as the carrier gas 1 ml/min) as described previously (25-26). Briefly, static HS injection was performed with a 1-µl injection volume, and a capillary column (Agilent, DB×5.625, 30 m×0.25 mm I.D.) was used for separation. Data analysis was performed with the PerkinElmer TotalChrom Workstation V.6.3.2 Data System.

Glucose consumption and ethanol fermentation values were calculated and expressed in DCM units (mg/kg). The glucose consumption and ethanol production by dry biomasses were determined in three independent experiments and mean±standard deviation values were calculated.

179

180 **Determination of intracellular metal contents of C*andida albicans* cells**

181 The culturing of fungal cells and surfactin treatment was performed as described above.
182 *Candida* cells were collected by centrifugation (5 min, 4 000×g, 4°C) after 4 hours of
183 incubation following surfactin exposure. The intracellular metal (Fe, Zn, Cu, and Mn)
184 contents of the dry biomass were measured by inductively coupled plasma optical emission
185 spectrometry (ICP-OES; 5110 Agilent Technologies, Santa Clara, CA, USA) following
186 atmospheric wet digestion in 3 ml of 65% HNO_3 and 1 ml of 30% H_2O_2 in glass beakers. The
187 metal contents of the samples were calculated in DCM units (in milligrams per kilogram)
188 using the method reported by Jakab et al. (23). The metal contents of the dry biomass were
189 determined in triplicate and mean±standard deviation values were calculated.

190

191 **Reactive species and glutathione production caused by surfactin exposure**

192 Reactive species were determined with or without 1 hour of surfactin exposure (128 mg/l) by
193 a reaction that converts 2′,7′-dichlorofluorescin diacetate to 2′,7′-dichlorofluorescein (DCF)
194 (Sigma, Budapest, Hungary) (19). The amount of DCF produced is proportional to the
195 quantity of reactive species.

196 Following a 4-hour surfactin exposure, reduced glutathione (GSH) and oxidized glutathione
197 (GSSG) contents were measured with 5,5′-dithio-bis (2-nitrobenzoic acid)-glutathione
198 reductase assay in cell-free yeast extracts prepared by 5-sulfosalicylic acid treatment as
199 described by Emri et al. (27).

200 Reactive species, GSH and GSSG were measured in three independent experiments and are
201 presented as means±standard deviation.

202

Adherence of *Candida albicans* cells to inert surface and the metabolic activity of adhered fungal cells over time

The density of the *Candida* suspension used in this experiment was $1x10^6$ CFU/ml. A total of 100 µl of the *C. albicans* suspension was pipetted into 96-well flat-bottom polystyrene microtitre plates (TPP, Trasadingen, Switzerland) in the presence of 128 mg/l surfactin and incubated statically at 37°C. Pre-determined wells were assigned to endpoints of 2, 4, 6, 8, 10, 12 and 24 hours. After 2, 4, 6, 8, 10, 12 and 24 hours, the corresponding pre-assigned wells were washed three times with sterile physiological saline then the metabolic activity of adhered cells was measured using the XTT-assay as described previously (19). The percent change in metabolic activity was calculated on the basis of the absorbance (*A*) at 492 nm as $100\%\times(A_{well}-A_{background})/(A_{drug\text{-}free\ well}-A_{background})$. Three independent experiments were performed and the mean ± standard deviation was calculated for each examined time point. Statistical comparisons of relative metabolic activity data were performed using the paired Student's *t* test. The differences between values for treated and control cells were considered significant if the *p* value was <0.05.

Adherence of *Candida albicans* cells to Caco-2 epithelial cells

For adhesion-related experiments, 1×10^5 epithelial cells were seeded on glass coverslips (pre-treated with rat tail derived collagen I; Gibco—Thermo Fisher, USA), placed in 24-well plates and incubated for 3 days prior to infection (28). For infection, pre-cultured *C. albicans* cells were collected by centrifugation (5 min, 4000×g, 4°C), washed three times with sterile physiological saline and adjusted to 2×10^5 cells/ml in DMEM. Fungal cells were co-incubated with Caco-2 epithelial cells for 1 hour in serum-free DMEM with or without 128 mg/l surfactin at 37°C in the presence of 5% CO_2. After co-incubation of epithelial cells with *C. albicans* cells, non-adherent yeast cells were removed by washing three times with sterile

228 physiological saline and the cells on the cover slips were fixed with 4% formaldehyde.
229 Adherent fungal cells were stained with calcofluor white (CFW; Merck, Budapest, Hungary)
230 and were visualized with a fluorescence microscope (Zeiss Axioskop 2 mot microscope
231 coupled with a Zeiss Axiocam HRc camera) (28). The number of adherent cells was
232 determined by counting at least 50 fields. Adhesion (%) was calculated using the following
233 formula: [(average cell count in the field area of the well in μm^2)/(area of the field in μm^2
234 inoculated yeast cells in each well)]×100 (28).
235 Statistical analysis was performed between control and surfactin-treated cultures using the
236 paired Student's *t* test. Significance was defined as a *p* value of < 0.05.
237
238 **Interactions between fluconazole and surfactin *in vitro***
239 Interactions between fluconazole and surfactin were examined using a two-dimensional broth
240 microdilution chequerboard assay. Interactions were analyzed by calculating the fractional
241 inhibitory concentration index (FICI) and using the Bliss independence model (29).
242 Interactions were determined in three independent experiments. The tested concentrations
243 ranged from 0.004 to 1 mg/l for fluconazole and from 4 to 256 mg/l for surfactin. FICIs were
244 determined using the following formula:
245 $\Sigma FIC=FIC_A+FIC_B=[(MIC_A^{comb}/MIC_A^{alone})]+[(MIC_B^{comb}/MIC_B^{alone})]$, where MIC_A^{alone} and
246 MIC_B^{alone} stand for the MICs of drugs A and B when used alone, and MIC_A^{comb} and MIC_B^{comb}
247 represent the MICs of drugs A and B in combination at isoeffective combinations,
248 respectively. FICIs were determined as the lowest ΣFIC. The MICs of the drugs alone and of
249 all combinations were determined as the lowest concentration resulting in at least a 50%
250 decrease in turbidity compared to the unexposed control cells. If the obtained MIC was higher
251 than the highest tested drug concentration, the next highest twofold concentration was
252 considered the MIC value. FICIs ≤ 0.5 were defined as synergistic, between > 0.5 and 4 as

253 indifferent, and > 4 as antagonistic (19, 29).

254 Fluconazole and surfactin interactions were further analyzed using the Bliss independence
255 model with help of the open access Synergyfinder ® application. Briefly, in this software, the
256 Bliss independence model compares the observed versus predicted inhibition response, where
257 a mean synergy score of less than -10 is considered antagonistic, between -10 and 10 is
258 considered to be indifferent and above 10 is synergistic (30).

259

260 **RNA sequencing**

261 For RNA extraction, fungal cells were collected 1 hour following surfactin exposure by
262 centrifugation (5 minutes, 4,000×g at 4°C). Fungal cells were washed three times with
263 phosphate-buffered saline (PBS) and stored at −70°C until examination. Total RNA samples
264 were prepared from lyophilized cells (CHRIST Alpha 1-2 LDplus lyophilizer, Osterode,
265 Germany) derived from untreated and surfactin-exposed cultures (22-23). Three independent
266 cultures were used for RNA-seq experiments and RT-qPCR tests. The quality of RNA was
267 determined using the Eukaryotic Total RNA Nano kit (Agilent, USA) in an Agilent
268 Bioanalyzer. RNA-Seq libraries were prepared from total RNA using an Ultra II RNA Sample
269 prep kit (New England BioLabs) according to the manufacturer's protocol. The single read
270 75-bp sequencing reads were generated on an Illumina NextSeq500 instrument.
271 Approximately 23–27 million reads were generated per sample. RNA-Seq libraries were
272 made by the Genomic Medicine and Bioinformatics Core Facility of the Department of
273 Biochemistry and Molecular Biology, Faculty of Medicine, University of Debrecen, Hungary.
274 Raw reads were aligned to the reference genome
275 (https://www.ncbi.nlm.nih.gov/genome/?term=Candida+albicans+SC5314), and the
276 percentage of aligned reads varied between 92% and 95% in each sample. Gene transcription
277 differences between surfactin-treated and control groups were compared using a moderated *t*

278 test; the Benjamini-Hochberg false discovery rate was used for multiple-testing correction,
279 and a corrected *P* value of <0.05 was considered significant. Up- and down-regulated genes
280 were defined as differentially expressed genes with >1.5-fold change (FC, up-regulated
281 genes) or less than -1.5-FC (down-regulated genes). The FC ratios were calculated from the
282 normalized gene transcription values.
283
284 **Reverse transcription quantitative real-time PCR (RT-qPCR) assays**
285 Surfactin-induced changes in the transcription of certain membrane transport, virulence and
286 primary metabolism genes were validated by RT-qPCR (22-23). The RT-qPCRs were
287 performed with a Luna Universal one-step RT-qPCR kit (NEB, USA) according to the
288 manufacturer's protocol using 500 ng of DNase (Merck, Budapest, Hungary)-treated total
289 RNA per reaction. Oligonucleotide primers (Table S1) were designed using Oligo Explorer
290 (version 1.1.) and Oligo Analyzer (version 1.0.2) software. Three parallel measurements were
291 performed for every sample in a LightCycler 96 real-time PCR instrument (Roche,
292 Switzerland). Relative transcription levels (ΔΔCP value) were determined based on the
293 following formula: $\Delta CP_{control} - \Delta CP_{treated}$ where $\Delta CP_{control} = CP_{tested\ gene,\ control} - CP_{reference\ gene,\ control}$
294 for untreated cultures, while $\Delta CP_{treated} = CP_{tested\ gene,\ treated} - CP_{reference\ gene,\ treated}$ for surfactin-
295 treated cultures. The CP values represent the RT-qPCR cycle numbers of crossing points.
296 Two reference genes (*TUB1* and *HPT1*) were tested. All showed stable transcription in our
297 experiments and, hence, only data relative to the *HPT1* (C2_02740C) transcription values are
298 presented.
299
300 **Gene set enrichment analysis**
301 Gene set enrichment analyses on the up-regulated and down-regulated gene sets were carried
302 out with the *Candida* Genome Database Gene Ontology Term Finder

(http://www.candidagenome.org/cgi-bin/GO/goTermFinder) using function, process, and component gene ontology (GO) terms. Only hits with a *p* value of <0.05 were considered during the evaluation process (Table S2).

Besides defined GO terms, groups of functionally related genes were also generated by extracting data from the *Candida* Genome Database (http://www.candidagenome.org) unless otherwise indicated (Table S3). The enrichment of *C. albicans* genes from these gene groups in the up-regulated and down-regulated gene sets was tested with Fisher's exact test ($p < 0.05$). The following gene groups were created:

(i) Virulence-related genes – Genes involved in the genetic control of *C. albicans* virulence were collected according to Mayer et al. (2013), Höfs et al. (2016) and Araújo et al. (2017) (31-33).

(ii) Antioxidant enzyme-related genes – This gene group includes genes encoding functionally verified and/or putative antioxidant enzymes according to catalase (GOID:4096), SOD (GOID:4784), glutaredoxin (GOID:6749), thioredoxin (GOIDs:8379 and 51920) and peroxidase (GOID:4601) GO terms.

(iii) Metabolic pathway-related genes – This group contains all genes related to the carbohydrate, ergosterol and fatty acid biochemical pathways according to the pathway databases (http://pathway.candidagenome.org/).

(iv) Metal metabolism-related genes – Genes involved in iron, zinc, copper and manganese acquisition by *C. albicans* were grouped according to Fourie et al. (2018) and Gerwien et al. (2018) (34-35).

Data availability

326 The data shown and discussed in this paper have been deposited in the NCBI Gene
327 Expression Omnibus (GEO) (36) (https://www.ncbi.nlm.nih.gov/geo/) with the following
328 accession no.: GSE199383
329

Results

Effects of surfactin on growth, morphology, and extracellular phospholipase, proteinase and esterase production by *Candida albicans*

The growth of *C. albicans* was examined following preculturing for 4 hours and subsequently treating with 128 mg/l surfactin in YPD medium. Growth was significantly inhibited within 1 hour after the addition of surfactin as assessed both by observed absorbance values (0.96±0.04 and 0.75±0.02 for untreated control and surfactin-exposed cells, respectively, at OD_{640}) ($p<0.001$) (Figure 1A) and DCM changes (0.95±0.1 g/l and 0.6±0.15 g/l for untreated control and surfactin-treated cells, respectively) ($p<0.01$) (Figure 1B). The observed growth inhibition was further confirmed by changes in measured DCM after 6 hours (1.5±0.2 g/l and 0.7±0.1 g/l) and 8 hours of incubation (3.2±0.3 g/l and 1.0±0.2 g/l) for untreated control and surfactin-exposed cells, respectively ($p<0.01$ to 0.001) (Figure 1B).

The type and ratio of filamentous morphological forms (hypha or pseudohypha) differed significantly compared to the yeast form in treated and untreated cultures. The ratio of hyphae and pseudohyphae was statistically comparable at 5 and 6 hours both for surfactin-treated and control cultures. However, the ratio of hyphae was significantly lower in surfactin-exposed culture compared with untreated cells from 8 hours of incubation (10.33%±2.08% vs. 14.33%±1.53%) ($p<0.05$). Furthermore, the ratio of pseudohyphae was 29.66%±3.06% and 22.67%±3.05% at 8 hours for treated and untreated cells, respectively ($p<0.05$) (Figure 1C).

Testing virulence-related enzymes revealed that surfactin treatment did not significantly influence the extracellular phospholipase (Pz values were 0.6±0.05 and 0.57±0.04), the aspartate proteinase (0.78±0.09 and 0.77±0.09) or the esterase activity (0.63±0.04 and 0.67±0.06) of *C. albicans* when compared with the untreated control cells.

Surfactin exposure significantly influences glucose consumption, ethanol production, and the intracellular metal contents of *Candida albicans* cells

The concentration of glucose consumption and ethanol fermentation of *C. albicans* was determined for 2 and 4 hours subsequently after surfactin exposure. Surfactin treatment caused a significant increase in glucose utilization at 4 hours post-exposure (4.1±0.3 g/g vs. 2.95±0.4 g/g DCM) (p<0.001) (Figure 2A). Enhanced ethanol fermentation was observed both at 2 hours (7.8±2.2 g/g DCM vs. 0.3±0.1 g/g DCM) (p<0.01) and 4 hours post-exposure (5.1±0.7 g/g DCM vs. 0.64±0.08 g/g DCM) (p<0.001) (Figure 2B).

Following 4 hours of surfactin treatment, the iron, manganese and zinc content of yeast cells decreased (70.9±8.4 mg/kg vs. 127.1±18.4 mg/kg, 5.3±1.3 mg/kg vs. 8.1±0.5 mg/kg, and 169.6±8.9 mg/kg vs. 214.4±4.5 mg/kg, for iron, manganese, and zinc in treated versus non-treated cells, respectively) (p<0.05 to 0.01), while the copper content of *C. albicans* cells did not differ significantly from the untreated control cultures (3.1±0.95 mg/kg vs. 2.0±0.25 mg/kg) (p>0.05) (Table 1).

Surfactin exposure increased the intracellular glutathione concentration of *Candida albicans* cells

Surfactin treatment did not enhance oxidative stress in *C. albicans* cells. DCF production as a marker of redox imbalance in the surfactin-treated cultures did not differ significantly from that observed in untreated control cultures (12.9±2.7 nmol DCF/OD_{640} and 11.5±1.8 nmol DCF/OD_{640}, respectively) (p>0.05). Nevertheless, the GSH concentration was significantly higher in the surfactin-challenged cells (37.2±10.4 nmol/mg vs. 2.05±0.8 nmol/mg) (p<0.01) than in untreated control cells, while surfactin treatment did not result in a significantly higher GSSG level (0.05±0.01 nmol/mg vs. 0.03±0.007 nmol/mg) (p>0.05).

Surfactin exposure inhibits the adhesion of *Candida albicans* to inert surface and to Caco-2 cells

The metabolic activity of inert surface-adhered *C. albicans* cells is depicted in Figure S1. In the first 12 hours, the relative metabolic activity of surfactin-exposed cells was significantly lower than that of the untreated control (p<0.01-0.001). Noticeably, the lowest metabolic activity was observed at 6 hours (48.07%±4.25%).

Adhesion of fungal cells to Caco-2 cells was significantly lower already 1 hour post surfactin exposure (2.2%±0.8% adherent cells) compared with untreated control cells (5.8%±1.1% adherent cells) (p<0.01).

Surfactin enhances the *in vitro* activity of fluconazole against *Candida albicans*

The nature of the interaction between surfactin and fluconazole was evaluated using FICI calculation and the BLISS independence model. Based on three independent experiments, the median MIC values for fluconazole and surfactin were 0.125 mg/l (0.125–0.25 mg/l) and >256 mg/l (256 to >256 mg/l) when added separately, while 0.004 mg/l and 8 mg/l (8–32 mg/l) in combination, respectively. A synergistic interaction between fluconazole and surfactin was observed for all three independent experiments, with FICI ranging from 0.135 to 0.37. The FICI values were clearly confirmed by the Bliss independence model, where the mean synergy score was 22.7 (Figure S2).

Transcriptional profiling and RNA-Seq data validation

Principal component analysis (PCA) and hierarchical clustering were used to represent visually the transcriptomic differences between samples treated with surfactin and the untreated controls. Analyses of the RNA sequencing data clearly indicated that surfactin has a

403 remarkable effect on *C. albicans* gene expression, leading to significant alterations in the
404 transcriptome (Figure S3).
405 Comparison of the surfactin-treated *C. albicans* global gene expression profile with that of
406 unexposed cells revealed 1389 differentially expressed genes. Among those, 773 were up-
407 regulated and 617 were down-regulated in the surfactin-exposed samples compared to the
408 untreated controls (Figure 3A–C, Figure 4, Tables S2 and S3).
409
410 **Evaluation of surfactin-responsive genes**
411 To obtain an overall comprehensive insight into the molecular effect of surfactin, gene
412 ontology terms were assigned to all of the genes in the *C. albicans* reference genome; after
413 which, we compared the terms for both the down-regulated and up-regulated genes with a
414 background of all terms.
415
416 *Virulence-related genes*
417 In agreement with reduced surface adhesion (see above), biofilm-related genes were
418 significantly enriched within the surfactin-responsive down-regulated gene group according
419 to Fisher's exact test (Table S3). Nine genes are involved in biofilm adhesion (*EAP1* and
420 *PGA1*), biofilm maturation (*EFG1*, *ROB1*, *CPH2*, *IFD6*, *GCA1*, and *ADH5*), and biofilm
421 dispersion (*NRG1*) (Figure 3A–C, Figure 4, Table S3). Down-regulation of *PLB1* and *NRG1*
422 expression following surfactin treatment was supported by RT-qPCR data (Figure 4 and Table
423 S4).
424
425 *Oxidative stress-related genes*
426 Surfactin exposure increased the expression of glutathione metabolism-related genes (*GTT11*,
427 *GTT12*, *GTT13*, *GCS1*, *GST2*, *C5_01560C*, and *TTR*1) and flavodoxin-like protein (FLPs)

genes (*PST1*, *PST2*, and *C2_07070W*) as well as the *CIP1* gene, which encodes an environmental stress-induced protein (Figure 3A–C, Figure 4, Table S3).

Metabolic pathway-related genes

Surfactin treatment led to decreased expression of several genes involved in glycolysis (*PFK2*, *PFK1*, *FBA1*, *TPI1*, *PGK1*, *GPM2*, *CDC19*, *HXK2*, and *GAL4*), ethanol fermentation (*PDC11, ADH5,* and *ADH1*), trehalose metabolism (*TPS1, TPS2, TPS3, NTH1,* and *ATC1*), glycogen biosynthesis (*C1_01360C, GSY1, GLC3,* and *PGM2*), gluconeogenesis (*MAE1, PCK1, GPM2, PGK1*, and *FBA1)*, ergosterol biosynthesis (*ERG1, ERG3, ERG9, ERG10,* and *ERG11*) and fatty acid biosynthesis (*ACC1, FAS1,* and *FAS2*) (Figure 3A–C, Figure 4, Table S3).

In addition, surfactin exposure caused a significant increase in the expression of preribosome biogenesis-related genes, including small subunit genes (*BUD21*, *BUD23*, *RPS27A*, *SAS10*, *DBP8* etc.) and large subunit genes (*CSI2*, *DBP3*, *SDA1*, *SPO22*, *YTM1* etc.)

Genes involved in iron homeostasis including ferric reductases (*CFL4, CFL11, CR_07300W, C7_00430W, FRE7,* and *FRE9)*, multicopper oxidases (*FET99* and *CCC2*), siderophore transport *(SIT1*), and *SEF1* transcription factor as well as copper homeostasis (*MAC1* encoding transcription factor*, CCS1, CTR1,* and *CCC2* coding for chaperone and copper transporters) and zinc metabolism (*CSR1* and *PRA1* encoding transcription factor and cell surface protein) were enriched in the up-regulated gene set (Figure 3A–C, Figure 4, Table S3).

In addition, surfactin exposure decreased the expression of ferric permease genes (*FTR1* and *FTR2*), hemoglobin utilization-related genes (*HMX1, PGA10*, and *CSA1*) and the *AFT2* gene encoding a transcription factor as well as vacuolar iron (*SMF3*), copper (*CRP1*) and zinc (*ZRT1*) transporters (Figure 3A–C, Figure 4, Table S3).

453 The up-regulation of *FRE7*, *SIT1*, and *CTR1* and the down-regulation of *TPS2, PCK1, ERG1,*
454 and *FAS2* were additionally confirmed by RT-qPCR (Figure 4, Table S3).
455
456 *Transmembrane transport-related genes*
457 Surfactin treatment led to increased expression of several genes involved in transmembrane
458 transport, including 62 antifungal drug transporter (e.g. *MDR1* and *FLU1*) and 134
459 carbohydrate transporter (*HGT1, HGT10, HGT14, HGT18, HXT5, NAG3, SFC1, GAL102*
460 etc.) genes (Figure 3A–C, Figure 4, Table S3).
461 In addition, 10 genes related to rRNA export from the nucleus (*RPS3, RPS5, RPS10, RPS15,*
462 *RPS18, RPS19A, RPS21, RPS26A, RPS28B,* and *YST1*) were significantly enriched in the
463 down-regulated gene set (Figure 3A–C, Figure 4, Table S3).
464 From this above list, RT-qPCR measurements demonstrated that surfactin exposure caused a
465 significant increase in the expression of *MDR1* (ABC transporter) and *HGT1* (glucose
466 transmembrane transporter) in the treated cells (Figure 4 and Table S4).
467

Discussion

Commensal co-existence of *C. albicans* with its human host has been a well-known phenomenon for decades. However, several studies have demonstrated that gastrointestinal *C. albicans* colonization is one of the most important predisposing factors for life-threatening invasive *Candida* infections (1-3). Biosurfactant production by probiotic bacterial species or its use as an adjuvant in complementary therapy may prevent the overgrowth of *C. albicans* cells, which could significantly reduce the need for antifungal agents and the risk of resistance development (37). Based on recent *in vitro* findings, one of the most effective biosurfactants is surfactin, which was first described from *B. subtilis* ATCC 21332 and has potent antimicrobial, antitumoral and anticoagulant activities (38). Studies of surfactin focusing on anti-*Candida* activity are scarce; nevertheless, Biniarz et al. (2015) reported that the cell surface hydrophobicity and adhesion of *C. albicans* decreased by 20–60% and 80–90%, respectively following surfactin exposure (39). Similar results were observed with regard to the inhibition of adherence and biofilm development by Nelson et al. (18). However, the detailed physiological and transcriptional background of the preliminary antifungal activity caused by surfactin remained to be elucidated.

Our work reveals several roles for *B. subtilis* surfactin as a potent modulator of *C. albicans* metabolism, morphogenesis and susceptibility to traditional antifungal drugs. The detected growth inhibition can be attributed to the general down-regulation of numerous metabolism-related genes. Although glucose consumption was significantly higher in surfactin-exposed cells at 4 hours, prior to this time this value was lower compared with the control, which coincided with the measured reduction of metabolic activity in the case of surfactin-treated adhered fungal cells. Interestingly, ribosome biogenesis-related genes were significantly up-regulated by surfactin treatment. Ribosome biogenesis is closely linked to such cellular activities as growth and division (40). After transcription, both the small and large pre-

493 ribosomal subunits must be exported to the cytoplasm to allow ribosome maturation. Our GO
494 term enrichment analysis revealed that surfactin treatment up-regulates the transcription of
495 genes connected to RNA metabolism (220 genes) including the pre-ribosome-related genes;
496 furthermore, it down-regulates the genes of rRNA transport (10 genes), cytosolic ribosomal
497 proteins (69 genes) and translation (128 genes). These transcriptomic results suggest that the
498 reduced growth of *C. albicans* cells can be also attributed to the suspension of protein
499 synthesis under surfactin treatment (40) in addition to altering expression of genes connected
500 to metabolism.
501 Several ergosterol (*ERG1*, *ERG3*, *ERG9*, *ERG10*, *ERG11*) and fatty acid metabolism-related
502 genes (*ACC1*, *FAS1*, *FAS2*) were down-regulated, suggesting possible changes in the
503 structure and fluidity of the cell membrane. The observed synergistic interaction between
504 surfactin and fluconazole supports these presumed membrane changes (41). Surprisingly, a
505 remarkable increase in ethanol content was detected in surfactin-exposed cultures both at 2
506 and 4 hours compared to the untreated control. Similarly, *Pseudomonas aeruginosa*-derived
507 phenazines increase the production of fermentation products such as ethanol by 3- to 5-fold in
508 *C. albicans* (42). Presumably, surfactin possibly shapes the chemical ecology of mixed-
509 species microbial communities. *C. albicans* biofilm development may also be influenced by
510 this elevated ethanol content, which has been shown to inhibit biofilm formation (43).
511 Moreover, transcription of both *EFG1* and *ECE1* were down-regulated, explaining the
512 inhibition of hyphae formation and biofilm development (44). A surfactin-diminished biofilm
513 production may potentially explain its probable interfering effect with fungal quorum sensing.
514 A previous studies highlighted that surfactin might act as a signal molecule in a paracrine
515 signaling cascade of *B. subtilis* (45). Furthermore, surfactin might also be involved in
516 interaction of *B. subtilis* with the black mold fungus, *Aspergillus niger*, resulting in altered
517 metabolism both in the bacterium and the fungus (46). Our data suggest that surfactin may

518 significantly influence the farnesol-mediated quorum sensing pathways in *C. albicans*
519 because farnesol synthesis was disturbed by the surfactin-induced down-regulation of the
520 lipid pyrophosphatase enzyme encoding *DPP2* (47). Tyrosol production may also be
521 disrupted based on the down-regulated level of *ADH1* and *ADH5*, both of which are involved
522 in tyrosine-tyrosol conversion in *C. albicans*, further explaining the observed inhibition of
523 biofilm formation (48). Regarding the inter-species interaction on biofilm formation, Liu et al.
524 (2019) reported the extensive inhibition of quorum sensing-related pathways by surfactin,
525 including biofilm formation by *Staphylococcus aureus* (49). Based on their findings, surfactin
526 has a significant effect on polysaccharide production and decreases the level of alkali-soluble
527 polysaccharide in biofilms (49).
528 The here obtained transcriptomic data highlighted that surfactin treatment significantly
529 influenced the transcription of iron metabolism, copper transport and zinc transport-related
530 genes as well as the intracellular iron, zinc and manganese contents of *C. albicans*. Notably,
531 similar consequences were observed in the case of *C. auris* following farnesol exposure (23).
532 The decreased iron content may be part of the general defense against surfactin to minimize
533 the damage caused by ferrous ions (50). In previous studies, the elevated level of free
534 intracellular iron facilitated the production of reactive oxygen species and triggered iron-
535 dependent cell death in *Saccharomyces cerevisiae* (51). The surfactin-induced reduction in
536 intracellular zinc content was associated with the down-regulation of the *ZRT2* gene, which
537 encodes the major zinc importer in *C. albicans*. Zinc is a crucial essential element in oxidative
538 stress defense as a structural component of superoxide dismutase; furthermore, *ZRT2* deletion
539 or down-regulation impaired virulence by decreasing the colonization rate of *C. albicans* and
540 reducing kidney fungal burden in a mouse infection model (52).
541 Copper homeostasis is also an important determinant for virulence in *C. albicans*. In our
542 work, transcription of *CTR1* was up-regulated simultaneously with the *FRE7* gene. Khemiri et

al. (2020) reported that under copper deprivation, *C. albicans*-activated genes required for copper uptake included the transporter Ctr1 and the ferric reductases Fre7 (52). At the same time, transcription of *CRP1* was down-regulated, which encodes a P-type ATPase that functions as a copper extrusion pump to facilitate survival in high copper environments (52). We hypothesize that surfactin binds to Cu^{2+} ions, mimicking copper deprivation. A previous study showed that Cu^{2+} ions preferentially bind to amide nitrogens of lipopeptide biosurfactants such as *B. subtilis*-derived surfactin (53).

Based on our data, surfactin did not generate elevated levels of reactive oxygen species. Nevertheless, GSH was significantly increased upon surfactin treatment. Studies in *C. albicans* suggest involvement of GSH in the yeast to mycelium morphological switching (54). The elevated GSH level is associated with inhibition of hyphae formation. Furthermore, the overproduction of GSH may induce reductive stress response explaining partly the observed inhibition (54). Presumably, surfactin can become conjugated to GSH during attempts to inactivate it and remove it from fungal cells, thus minimizing the damage caused by this compound. Importantly, the transcription level of the gene encoding the Mdr1-P-glycoprotein was significantly up-regulated, further suggesting its role in surfactin detoxification (55).

In summary, this is the first study examining the changes in gene transcription in *C. albicans* following surfactin exposure. Surfactin decreased the adherence of fungal cells, modulated the morphology toward yeast and pseudohyphae forms, and inhibited biofilm formation. Moreover, surfactin significantly repressed the expression of ergosterol synthesis-related genes and major metabolic pathways. It also reduced iron, manganese and zinc metabolism, but significantly enhanced ethanol production. Focusing on its potential applicability as an adjuvant or probiotic-derived compound, the most important advantages of surfactin are its low risk of toxicity, high biodegradability properties and long-term physico-chemical stability. Nevertheless, two major limitations should be highlighted. Biotechnological

568 processes including the synthesis of surfactin are currently relatively expensive and
569 optimization of the purification process may be problematic. Furthermore, the extent of the
570 available data focusing on *in vivo* experiments is limited. Nonetheless, there is huge potential
571 for surfactin and surfactin-producing microbes, especially against gastrointestinal candidiasis,
572 and it would be a mistake to leave this potential untapped.

573

574 Conflict of interest

575 L. Majoros received conference travel grants from MSD, Astellas and Pfizer. All other
576 authors declare no conflicts of interest.

577

578 Funding

579 R. Kovács was supported by the Janos Bolyai Research Scholarship of the Hungarian
580 Academy of Sciences. This research was supported by the Hungarian National Research,
581 Development and Innovation Office (NKFIH FK138462). R. Kovács was supported by the
582 UNKP-21-5-DE-473 New National Excellence Program of the Ministry for Innovation and
583 Technology from the Source of the National Research, Development and Innovation Fund.
584 The work is supported by the GINOP-2.3.4-15-2020-00008 project. The project is co-
585 financed by the European Union and the European Regional Development Fund. Secondary
586 metabolite-related projects in the group of Á.T. Kovács is funded by the Danish National
587 Research Foundation (DNRF137) for the Center for Microbial Secondary Metabolites.

588

589 Ethical approval

590 Not required

591

592

References

1. Miranda LN, van der Heijden IM, Costa SF, Sousa AP, Sienra RA, Gobara S, Santos CR, Lobo RD, Pessoa VP Jr, Levin AS. 2009. Candida colonisation as a source for candidaemia. J Hosp Infect 72:9-16. doi: 10.1016/j.jhin.2009.02.009.

2. Alonso-Monge R, Gresnigt MS, Román E, Hube B, Pla J. 2021. Candida albicans colonization of the gastrointestinal tract: A double-edged sword. PLoS Pathog 17:e1009710. doi: 10.1371/journal.ppat.1009710.

3. Zaborin A, Smith D, Garfield K, Quensen J, Shakhsheer B, Kade M, Tirrell M, Tiedje J, Gilbert JA, Zaborina O, Alverdy JC. 2014. Membership and behavior of ultra-low-diversity pathogen communities present in the gut of humans during prolonged critical illness. mBio 5:e01361-14. doi: 10.1128/mBio.01361-14

4. Matsubara VH, Bandara HM, Mayer MP, Samaranayake LP. 2016. Probiotics as Antifungals in Mucosal Candidiasis. Clin Infect Dis 62:1143-53. doi: 10.1093/cid/ciw038.

5. Hu L, Zhou M, Young A, Zhao W, Yan Z. 2019. In vivo effectiveness and safety of probiotics on prophylaxis and treatment of oral candidiasis: a systematic review and meta-analysis. BMC Oral Health 19:140. doi: 10.1186/s12903-019-0841-2.

6. Andrade JC, Kumar S, Kumar A, Černáková L, Rodrigues CF. 2021. Application of probiotics in candidiasis management. Crit Rev Food Sci Nutr. 22:1-16. doi: 10.1080/10408398.2021.1926905.

618 7. Elshaghabee FMF, Rokana N, Gulhane RD, Sharma C, Panwar H. 2017. Bacillus As
619 Potential Probiotics: Status, Concerns, and Future Perspectives. Front Microbiol 8:1490. doi:
620 10.3389/fmicb.2017.01490.
621
622 8. Jones SE, Paynich ML, Kearns DB, Knight KL. Protection from intestinal
623 inflammation by bacterial exopolysaccharides. 2014. J Immunol 192:4813-20. doi:
624 10.4049/jimmunol.1303369.
625
626 9. Jones SE, Knight KL. Bacillus subtilis-mediated protection from Citrobacter
627 rodentium-associated enteric disease requires espH and functional flagella. 2012. Infect
628 Immun. 80:710-9. doi: 10.1128/IAI.05843-11
629
630 10. Su Y, Liu C, Fang H, Zhang D. 2020. Bacillus subtilis: a universal cell factory for
631 industry, agriculture, biomaterials and medicine. Microb Cell Fact 19:173. doi:
632 10.1186/s12934-020-01436-8.
633
634 11. Arnaouteli S, Bamford NC, Stanley-Wall NR, Kovács ÁT. 2021. Bacillus subtilis
635 biofilm formation and social interactions. Nat Rev Microbiol. 19:600-614. doi:
636 10.1038/s41579-021-00540-9.
637
638 12. Kiesewalter HT, Lozano-Andrade CN, Wibowo M, Strube ML, Maróti G, Snyder D,
639 Jørgensen TS, Larsen TO, Cooper VS, Weber T, Kovács ÁT. 2021. Genomic and Chemical
640 Diversity of Bacillus subtilis Secondary Metabolites against Plant Pathogenic Fungi.
641 mSystems 6:e00770-20. doi: 10.1128/mSystems.
642

643 13. Devi S, Kiesewalter HT, Kovács R, Frisvad JC, Weber T, Larsen TO, Kovács ÁT,
644 Ding L. 2019. Depiction of secondary metabolites and antifungal activity of Bacillus
645 velezensis DTU001. Synth Syst Biotechnol. 4:142-149. doi: 10.1016/j.synbio.2019.08.002.
646
647 14. Georgiou G, Lin SC, Sharma MM. 1992. Surface-active compounds from
648 microorganisms. Biotechnology (N Y) 10:60-5. doi: 10.1038/nbt0192-60.
649
650 15. Ceresa C, Rinaldi M, Chiono V, Carmagnola I, Allegrone G, Fracchia L. 2016.
651 Lipopeptides from Bacillus subtilis AC7 inhibit adhesion and biofilm formation of Candida
652 albicans on silicone. Antonie Van Leeuwenhoek. 109:1375-88. doi: 10.1007/s10482-016-
653 0736-z.
654
655 16. Janek T, Drzymała K, Dobrowolski A. 2020. In vitro efficacy of the lipopeptide
656 biosurfactant surfactin-C15 and its complexes with divalent counterions to inhibit Candida
657 albicans biofilm and hyphal formation. Biofouling 36:210-221. doi:
658 10.1080/08927014.2020.1752370.
659
660 17. Suchodolski J, Derkacz D, Muraszko J, Panek JJ, Jezierska A, Łukaszewicz M,
661 Krasowska A. 2020. Fluconazole and Lipopeptide Surfactin Interplay During Candida
662 albicans Plasma Membrane and Cell Wall Remodeling Increases Fungal Immune System
663 Exposure. Pharmaceutics 12:314. doi: 10.3390/pharmaceutics12040314.
664
665 18. Nelson J, El-Gendy AO, Mansy MS, Ramadan MA, Aziz RK. 2020. The
666 biosurfactants iturin, lichenysin and surfactin, from vaginally isolated lactobacilli, prevent

667 biofilm formation by pathogenic Candida. FEMS Microbiol Lett 367:fnaa126. doi:
668 10.1093/femsle/fnaa126.
669
670 19. Nagy F, Vitális E, Jakab Á, Borman AM, Forgács L, Tóth Z, Majoros L, Kovács R.
671 2020. In vitro and in vivo Effect of Exogenous Farnesol Exposure Against Candida auris.
672 Front Microbiol 11:957. doi: 10.3389/fmicb.2020.00957.
673
674 20. Nemes D, Kovács R, Nagy F, Mező M, Poczok N, Ujhelyi Z, Pető Á, Fehér P,
675 Fenyvesi F, Váradi J, Vecsernyés M, Bácskay I. 2018. Interaction between Different
676 Pharmaceutical Excipients in Liquid Dosage Forms-Assessment of Cytotoxicity and
677 Antimicrobial Activity. Molecules 23(7):1827. doi: 10.3390/molecules23071827.
678
679 21. Al-Ajlani MM, Sheikh MA, Ahmad Z, Hasnain S. 2007. Production of surfactin from
680 Bacillus subtilis MZ-7 grown on pharmamedia commercial medium. Microb Cell Fact 6:17.
681 doi: 10.1186/1475-2859-6-17.
682
683 22. Jakab Á, Tóth Z, Nagy F, Nemes D, Bácskay I, Kardos G, Emri T, Pócsi I, Majoros L,
684 Kovács R. 2019. Physiological and Transcriptional Responses of Candida parapsilosis to
685 Exogenous Tyrosol. Appl Environ Microbiol 85:e01388-19. doi: 10.1128/AEM.01388-19.
686
687 23. Jakab Á, Balla N, Ragyák Á, Nagy F, Kovács F, Sajtos Z, Tóth Z, Borman AM, Pócsi
688 I, Baranyai E, Majoros L, Kovács R. 2021. Transcriptional Profiling of the Candida auris
689 Response to Exogenous Farnesol Exposure. mSphere 6(5):e0071021. doi:
690 10.1128/mSphere.00710-21.
691

692 24. Kantarcioglu AS, Yücel A. Phospholipase and protease activities in clinical Candida
693 isolates with reference to the sources of strains. 2002. Mycoses 45:160-5. doi:
694 10.1046/j.1439-0507.2002.00727.x.
695
696 25. Jakab Á, Emri T, Csillag K, Szabó A, Nagy F, Baranyai E, Sajtos Z, Géczi D, Antal K,
697 Kovács R, Szabó K, Dombrádi V, Pócsi I. 2021. The Negative Effect of Protein Phosphatase
698 Z1 Deletion on the Oxidative Stress Tolerance of Candida albicans Is Synergistic with
699 Betamethasone Exposure. J Fungi (Basel) 7:540. doi: 10.3390/jof7070540.
700
701 26. Diekmann JA 3rd, Cochran J, Hodgson JA, Smuts DJ. 2020. Quantitation and
702 identification of ethanol and inhalant compounds in whole blood using static headspace gas
703 chromatography vacuum ultraviolet spectroscopy. J Chromatogr A 1611:460607. doi:
704 10.1016/j.chroma.2019.460607.
705
706 27. Emri T, Pócsi I, Szentirmai A. 1997. Glutathione metabolism and protection against
707 oxidative stress caused by peroxides in Penicillium chrysogenum. Free Radic Biol Med
708 23:809–814.
709
710 28. Jakab Á, Mogavero S, Förster TM, Pekmezovic M, Jablonowski N, Dombrádi V,
711 Pócsi I, Hube B. 2016. Effects of the glucocorticoid betamethasone on the interaction of
712 Candida albicans with human epithelial cells. Microbiology 162:2116-2125. doi:
713 10.1099/mic.0.000383.
714
715 29. Meletiadis J, Verweij PE, TeDorsthorst DT, Meis JF, Mouton JW. 2005. Assessing in
716 vitro combinations of antifungal drugs against yeasts and filamentous fungi: comparison of

717 different drug interaction models. Med Mycol. 43:133-52. doi:
718 10.1080/13693780410001731547.
719
720 30. Robinson AGJ, Kanaan YM, Copeland RL. 2020. Combinatorial Cytotoxic Effects of
721 2,3-Dichloro-5,8-dimethoxy-1,4-naphthoquinone and 4-hydroxytamoxifen in Triple-negative
722 Breast Cancer Cell Lines. Anticancer Res. 40:6623-6635. doi: 10.21873/anticanres.14687.
723
724 31. Mayer FL, Wilson D, Hube B. 2013. Candida albicans pathogenicity mechanisms.
725 Virulence. 4:119-28. doi: 10.4161/viru.22913.
726
727 32. Höfs S, Mogavero S, Hube B. 2016. Interaction of Candida albicans with host cells:
728 virulence factors, host defense, escape strategies, and the microbiota. J Microbiol. 54:149-69.
729 doi: 10.1007/s12275-016-5514-0.
730
731 33. Araújo D, Henriques M, Silva S. 2017. Portrait of Candida Species Biofilm
732 Regulatory Network Genes. Trends Microbiol 25:62-75. doi: 10.1016/j.tim.2016.09.004.
733
734 34. Fourie R, Kuloyo OO, Mochochoko BM, Albertyn J, Pohl CH. 2018. Iron at the
735 Centre of Candida albicans Interactions. Front Cell Infect Microbiol 8:185. doi:
736 10.3389/fcimb.2018.00185.
737
738 35. Gerwien F, Skrahina V, Kasper L, Hube B, Brunke S. 2018. Metals in fungal
739 virulence. FEMS Microbiol Rev 42:fux050. doi: 10.1093/femsre/fux050.
740

741 36. Edgar R, Domrachev M, Lash AE. 2002. Gene Expression Omnibus: NCBI gene
742 expression and hybridization array data repository. Nucleic Acids Res 30:207-10. doi:
743 10.1093/nar/30.1.207.
744
745 37. Ouwehand AC, Forssten S, Hibberd AA, Lyra A, Stahl B. 2016. Probiotic approach to
746 prevent antibiotic resistance. Ann Med 48:246-55. doi: 10.3109/07853890.2016.1161232.
747
748 38. Morikawa M, Hirata Y, Imanaka T. 2000. A study on the structure-function
749 relationship of lipopeptide biosurfactants. Biochim Biophys Acta 1488:211-8. doi:
750 10.1016/s1388-1981(00)00124-4.
751
752 39. Biniarz P, Baranowska G, Feder-Kubis J, Krasowska A. 2015. The lipopeptides
753 pseudofactin II and surfactin effectively decrease Candida albicans adhesion and
754 hydrophobicity. Antonie Van Leeuwenhoek 108:343-53. doi: 10.1007/s10482-015-0486-3.
755
756 40. Shore D, Zencir S, Albert B. 2021. Transcriptional control of ribosome biogenesis in
757 yeast: links to growth and stress signals. Biochem Soc Trans 49:1589-1599. doi:
758 10.1042/BST20201136.
759
760 41. Bibi M, Murphy S, Benhamou RI, Rosenberg A, Ulman A, Bicanic T, Fridman M,
761 Berman J. 2021. Combining Colistin and Fluconazole Synergistically Increases Fungal
762 Membrane Permeability and Antifungal Cidality. ACS Infect Dis 7:377-389. doi:
763 10.1021/acsinfecdis.0c00721.
764

765 42. Morales DK, Grahl N, Okegbe C, Dietrich LE, Jacobs NJ, Hogan DA. 2013. Control
766 of Candida albicans metabolism and biofilm formation by Pseudomonas aeruginosa
767 phenazines. mBio 4:e00526-12. doi: 10.1128/mBio.00526-12.
768
769 43. Mukherjee PK, Mohamed S, Chandra J, Kuhn D, Liu S, Antar OS, Munyon R,
770 Mitchell AP, Andes D, Chance MR, Rouabhia M, Ghannoum MA. 2006. Alcohol
771 dehydrogenase restricts the ability of the pathogen Candida albicans to form a biofilm on
772 catheter surfaces through an ethanol-based mechanism. Infect Immun 74:3804-16. doi:
773 10.1128/IAI.00161-06.
774
775 44. Cavalheiro M, Teixeira MC. Candida Biofilms: Threats, Challenges, and Promising
776 Strategies. 2018. Front Med (Lausanne) 5:28. doi: 10.3389/fmed.2018.00028.
777
778 45. López D, Vlamakis H, Losick R, Kolter R. 2009. Paracrine signaling in a bacterium.
779 Genes Dev 23:1631-8. doi: 10.1101/gad.1813709.
780
781 46. Benoit I, van den Esker MH, Patyshakuliyeva A, Mattern DJ, Blei F, Zhou M,
782 Dijksterhuis J, Brakhage AA, Kuipers OP, de Vries RP, Kovács ÁT. 2015. Bacillus subtilis
783 attachment to Aspergillus niger hyphae results in mutually altered metabolism. Environ
784 Microbiol 17:2099-113. doi: 10.1111/1462-2920.12564.
785
786 47. Nickerson KW, Atkin AL. 2017. Deciphering fungal dimorphism: Farnesol's
787 unanswered questions. Mol Microbiol 103:567-575. doi: 10.1111/mmi.13601.
788

789 48. Ghosh S, Kebaara BW, Atkin AL, Nickerson KW. 2008. Regulation of aromatic
790 alcohol production in Candida albicans. Appl Environ Microbiol 74:7211-8. doi:
791 10.1128/AEM.01614-08.
792
793 49. Liu J, Li W, Zhu X, Zhao H, Lu Y, Zhang C, Lu Z. 2019. Surfactin effectively inhibits
794 Staphylococcus aureus adhesion and biofilm formation on surfaces. Appl Microbiol
795 Biotechnol 10:4565-4574. doi: 10.1007/s00253-019-09808-w.
796
797 50. Dixon SJ, Stockwell BR. 2014. The role of iron and reactive oxygen species in cell
798 death. Nat Chem Biol 10:9–17. https://doi.org/10.1038/nchembio.1416.
799
800 51. Bellotti D, Miller A, Rowińska-Żyrek M, Remelli M. 2022. Zn2+ and Cu2+ Binding
801 to the Extramembrane Loop of Zrt2, a Zinc Transporter of Candida albicans. Biomolecules.
802 12:121. doi: 10.3390/biom12010121.
803
804 52. Khemiri I, Tebbji F, Sellam A. 2020. Transcriptome Analysis Uncovers a Link
805 Between Copper Metabolism, and Both Fungal Fitness and Antifungal Sensitivity in the
806 Opportunistic Yeast Candida albicans. Front Microbiol 11:935. doi:
807 10.3389/fmicb.2020.00935.
808
809 53. Janek T, Rodrigues LR, Gudiña EJ, Czyżnikowska Ż. 2019. Metal-Biosurfactant
810 Complexes Characterization: Binding, Self-Assembly and Interaction with Bovine Serum
811 Albumin. Int J Mol Sci 20:2864. doi: 10.3390/ijms20122864.
812

813 54. Pócsi I, Prade RA, Penninckx MJ. 2004. Glutathione, altruistic metabolite in fungi.
814 Adv Microb Physiol 49:1-76. doi: 10.1016/S0065-2911(04)49001-8
815
816 55. van Haaften RI, Haenen GR, Evelo CT, Bast A. 2003. Effect of vitamin E on
817 glutathione-dependent enzymes. Drug Metab Rev 35:215-53.
818

819 **Table 1 Surfactin-induced iron, manganese, zinc, and copper content in *Candida***

820 ***albicans***

821

Metal contents/ Treatment	Mean value± SD [a]			
	Fe (mg/kg)	Mn (mg/kg)	Zn (mg/kg)	Cu (mg/kg)
Untreated cultures	127.1±18.4	8.1±0.5	214.4±4.5	2.0±0.25
Surfactin-treated cultures	70.9±8.4 *	5.3±1.3 *	169.6±8.9 **	3.1±0.95

822

823

824 [a] Mean values ± standard deviations (SD) calculated from three independent experiments are

825 presented.

826 *and ** indicate significant differences at p values of <0.05 and 0.01, respectively, calculated

827 by paired Student's t test, comparing untreated control and surfactin-treated cultures.

828

Figure Legends

Figure 1 Effect of surfactin on the growth and morphology transition of *Candida albicans*

Changes in the growth of *C. albicans* were examined by measurement of the absorbance (OD_{640}) (A) and dry cell mass (DCM) (B). Typical morphological forms can be observed in untreated and surfactin-exposed (SUR) *C. albicans* cultures at 4, 5, 6 and 8 hours (C). Following a 4-hour incubation, surfactin (SUR) was added at a final concentration of 125 mg/l to the YPD cultures. Data represent mean values with standard deviations (SD) calculated from three independent experiments. The asterisks indicate a statistically significant difference between control and surfactin-treated cultures calculated using the paired Student's *t* test (** $p < 0.01$, *** $p < 0.001$).

Figure 2 The physiological effect of surfactin exposure in *Candida albicans*

The physiological effects of surfactin exposure on glucose utilization (A) and ethanol production (B). Cell cultures were exposed to 128 mg/l surfactin (SUR) for 4 hours. Samples were taken after 2 and 4 hours of surfactin exposure. Data represent mean values ± standard deviation calculated from three independent experiments. *, ** and *** indicate significant differences at *p* values of <0.05, 0.01 and 0.001, respectively, calculated using the paired Student's *t* test, comparing untreated control and surfactin-treated cultures.

Figure 3 Overview of transcriptional changes induced by surfactin in *C. albicans*. Up-regulated (red) and down-regulated (blue) genes were defined as differentially expressed genes (corrected *p* value of <0.05), with more than a 1.5-fold increase or decrease in their transcription (surfactin treated versus untreated) (A).

Summary of gene enrichment analyses and the number of genes affected by *C. albicans* exposure to surfactin (B–C). The enrichment of up-regulated (B) and down-regulated (C) gene groups was identified using the Candida Genome Database Gene Ontology Term Finder (http://www.candidagenome.org/cgi-bin/GO/goTermFinder) or was tested by Fisher's exact test. The data sets for the gene groups are available in Tables S2 and Table S3 in the supplemental material.

Figure 4. The effects of surfactin on the expression of selected genes of *C. albicans*. The heat map demonstrates the expression profiles of representative genes according to the colour scale that indicates gene expression changes. Bold names indicate the genes that were selected for analysis by RT-qPCR. The data sets for the gene groups are available in Tables S2, Table S3 and Table S4 in the supplemental material.

Supplementary Figure S1 Changes in metabolic activity over time in *Candida albicans* adhered to an inert surface in the presence of 128 mg/l surfactin.

The untreated control cells showed 100% metabolic activity at each time point. Data represent mean values of relative metabolic activity ± standard deviation calculated from three independent experiments. Statistical analysis was performed using the paired Student's *t* test.

Supplementary Figure S2 The nature of interaction using the BLISS independence model

2D (A) and 3D (B) synergy maps demonstrate the combination landscape of fluconazole with surfactin. Synergy maps were generated using the open access "SynergyFinder" program.

878 **Supplementary Figure S3 Cluster (A) and principal component (B) analysis of the**
879 **transcriptome data.**

880 Symbols represent untreated control (Cont) and 128 mg/l surfactin-exposed (SUR) cultures.
881 The distribution of transcriptome data obtained in three independent series of experiments (I,
882 II, and III). Analyses were performed with the StrandNGS software using default settings.

883

884 **Supplementary Table S1 Oligonucleotide primers used for RT-qPCR analysis.**

885

886 **Supplementary Table S2 Results of the gene set enrichment analysis.**

887 Significant shared GO terms ($p < 0.05$) were determined with the Candida Genome Database
888 Gene Ontology Term Finder (http://www.candidagenome.org/cgi-bin/GO/goTermFinder).
889 Up- and down-regulated genes were defined as differentially expressed genes where $\log_2(FC)$
890 > 0.585 or $\log_2(FC) < -0.585$. The FC ratios were calculated from the normalized gene
891 expression values. Biological processes, molecular function and cellular component
892 categories are provided.

893

894 **Supplementary Table S3 Transcription data of selected gene groups.**

895 Part 1: Genes involved in genetic control of *Candida albicans* virulence.

896 Part 2: Genes involved in antioxidative defense.

897 Part 3: Genes involved in selected metabolic pathways.

898 Part 4: Genes or ergosterol and fatty acid metabolism.

899 Part 5: Genes involved in iron, zinc, copper and manganese metabolism.

900 Part 6: Genes involved in autophagy.

901 Part 7: Genes involved in apoptosis.

902 The systematic names, gene names and the features (putative molecular function or biological
903 process) of the genes are given according to the *Candida* Genome Database
904 (http://www.candidagenome.org).
905 Up- and down-regulated genes are marked with red and blue colour. Up- and down-regulated
906 genes were defined as differentially expressed genes with >1.5-fold change (FC, up-regulated
907 genes) or less than -1.5-FC (down-regulated genes) values. The FC ratios were calculated
908 from the normalized gene transcription values.
909 Results of gene enrichment analysis (Fisher's exact test) are also enclosed. "The response of
910 oxidative stress" genes (GOID: 0006979) collected from Gene Ontology Term Finder
911 (http://www.candidagenome.org/cgi-bin/GO/goTermFinder).
912
913 **Supplementary Table S4 Results of RT-qPCR experiments**
914 RNA-Seq data are presented as FC values, where FC is "fold change". Relative transcription
915 levels were quantified as $\Delta\Delta CP = \Delta CP_{control} - \Delta CP_{treated}$, where $\Delta CP_{treated} = CP_{tested\ gene} -$
916 $CP_{reference\ gene}$, measured from surfactin treated cultures, and $\Delta CP_{control} = CP_{tested\ gene} - CP_{reference}$
917 $_{gene}$, measured from control cultures. CP values represent the RT-qPCR cycle numbers of
918 crossing points. The *HPT1* gene was used as a reference gene. ΔΔCP values significantly
919 ($p < 0.05$ by Student's t test; $n = 3$) higher or lower than zero (up- or down-regulated genes)
920 are marked in red and blue, respectively. Pearson's correlation coefficient between the RT-
921 qPCR and RNA-Seq values was 0.95.

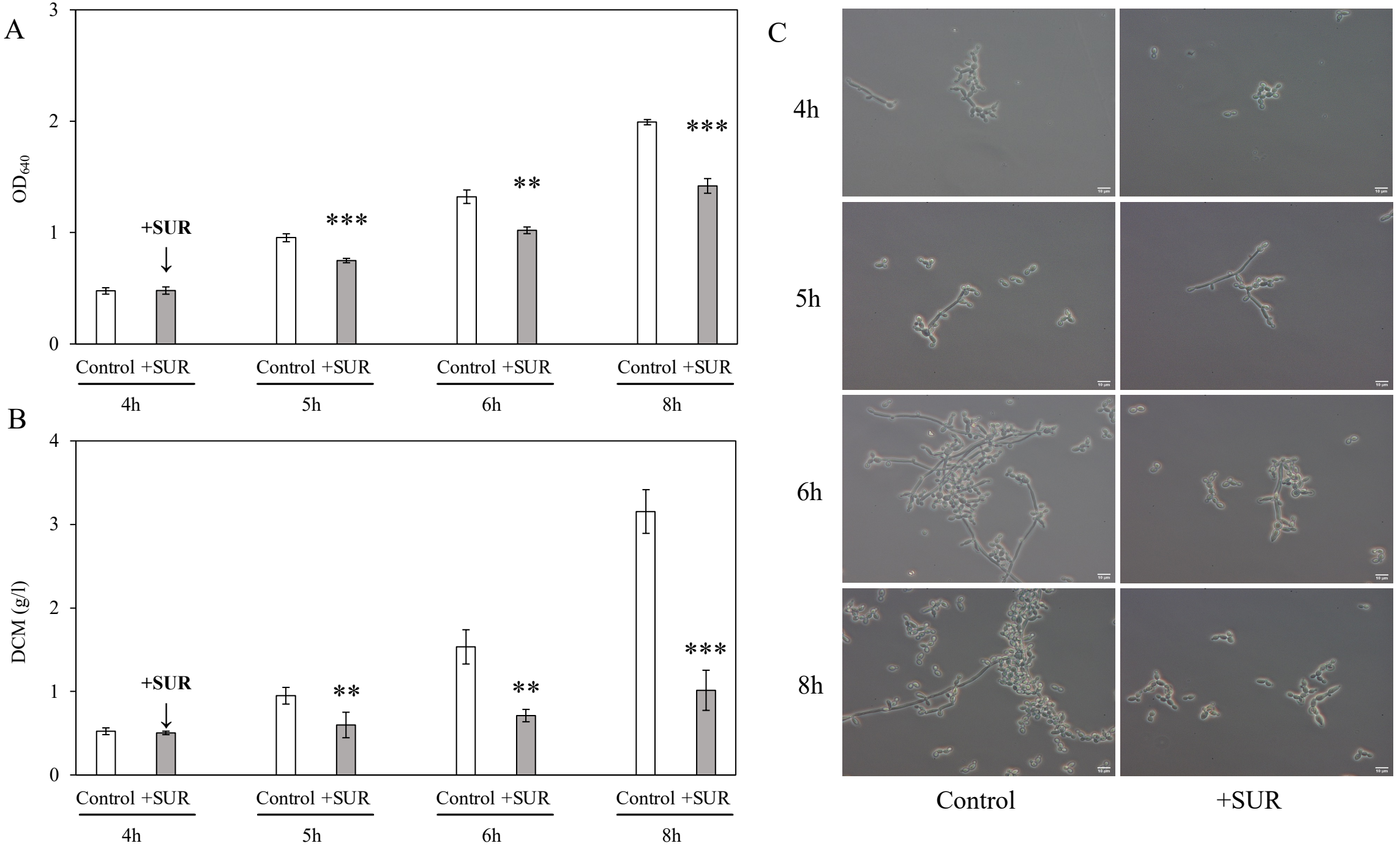
A
OD640
+SUR
***
**
***
Control +SUR
4h
5h
6h
8h
B
DCM (g/l)
+SUR
**
**
***
Control +SUR
4h
5h
6h
8h
C
4h
5h
6h
8h
Control
+SUR

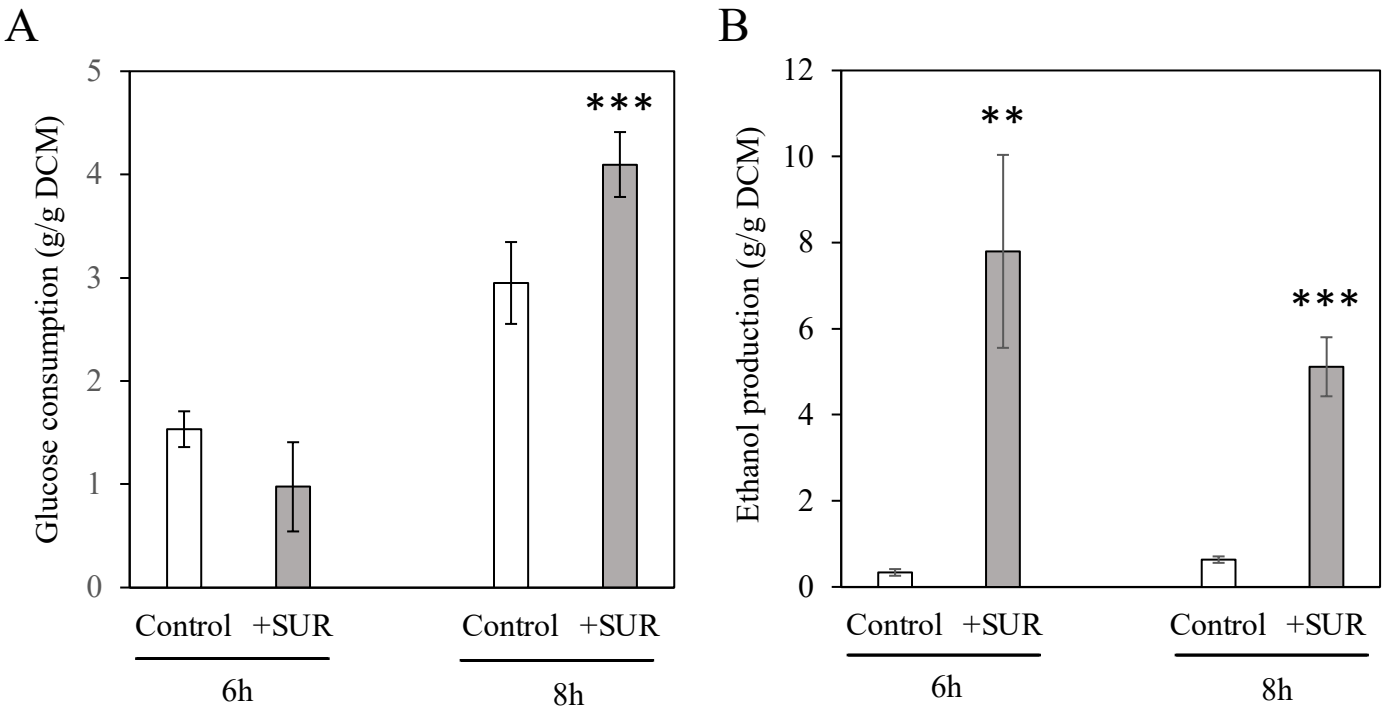
A
B
Glucose consumption (g/g DCM)
Ethanol production (g/g DCM)
0
1
2
3
4
5
0
2
4
6
8
10
12
***
**
***
Control
+SUR
Control
+SUR
Control
+SUR
Control
+SUR
6h
8h
6h
8h

A

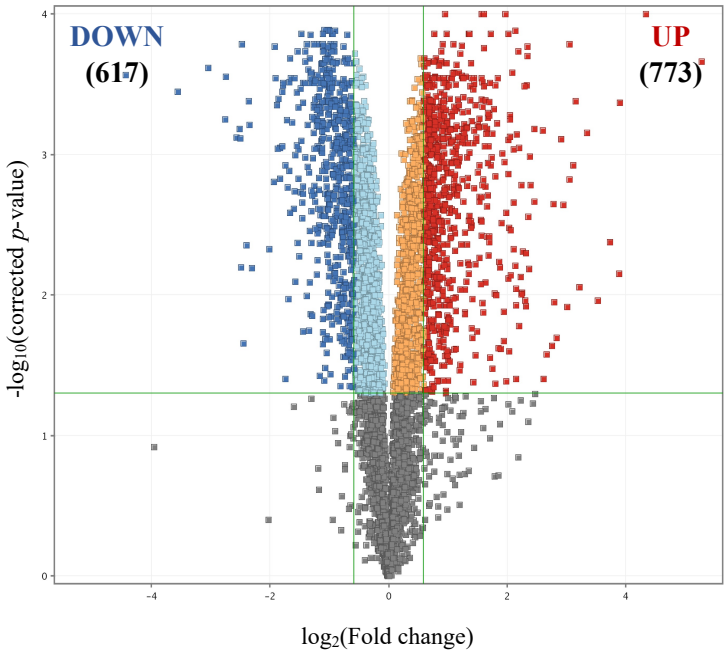

B

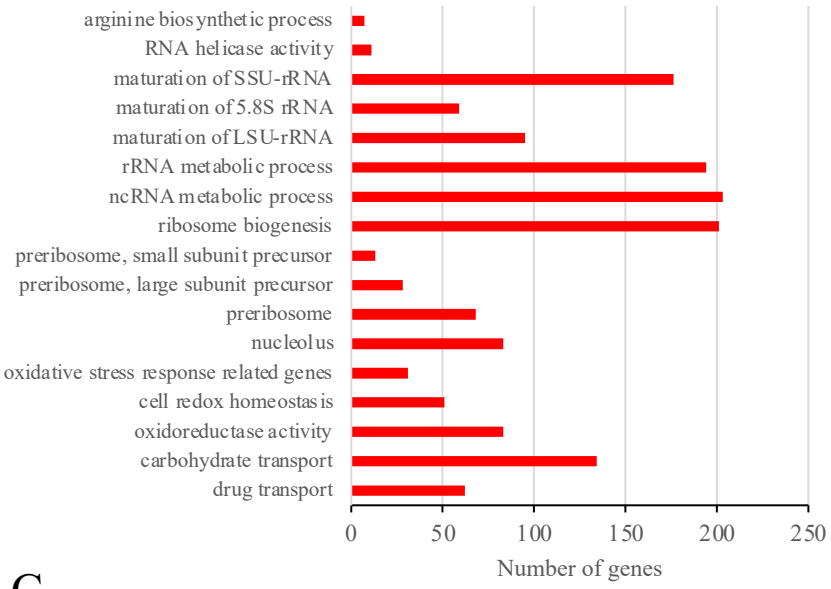

C